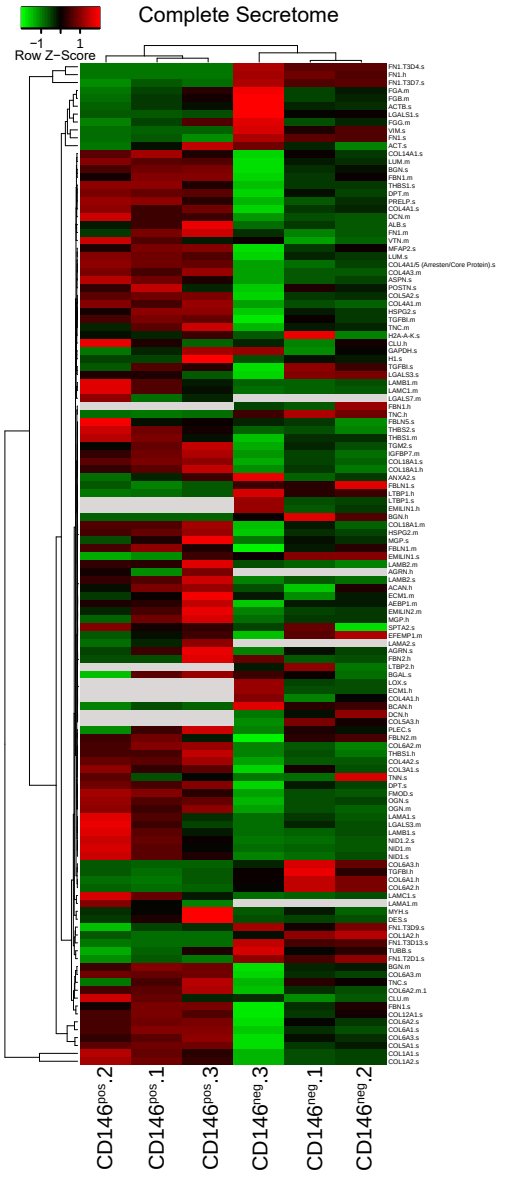

Supplemental Figure 1. The Complete TME Secretome. Heatmap illustrations show how tumors cluster according to CAF subtype by the Complete Secretome. Proteomics was completed in triplicate ($CD146^{pos}$.1-.3 and $CD146^{neg}$.1-.3). Low to high expression = green to red; grey indicates no expression.

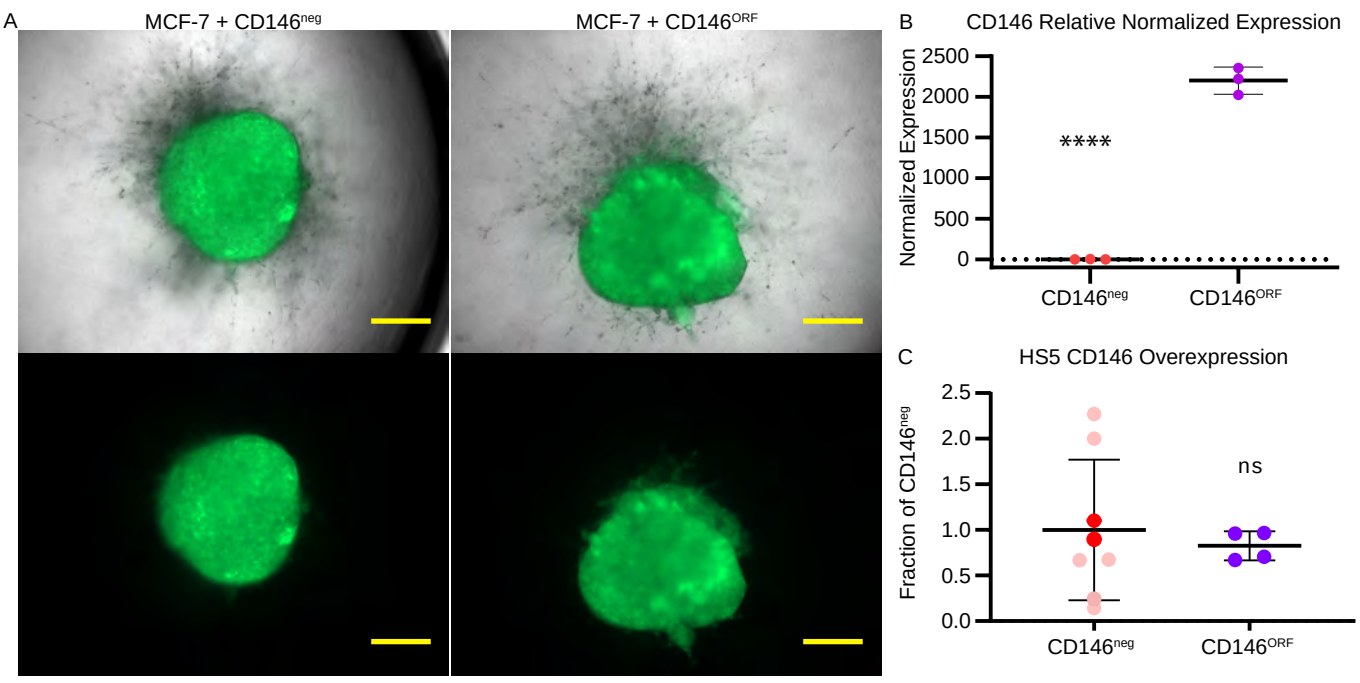

Supplemental Figure 2. MCF-7 invasion is not inhibited by CD146 over-expression in $CD146^{neg}$ CAFs. (A) $CD146^{neg}$ CAFs were generated to stably express CD146 ($CD146^{ORF}$) and grown in spheroid co-cultures with MCF-7 cells to determine if CD146 expression was responsible for invasion induced by $CD146^{neg}$ CAFs. (B) Generation of CD146 mRNA was verified by qPCR. (C) Quantification of MCF-7 cells mixed with native $CD146^{neg}$ CAFs (dark red dots) or $CD146^{neg}$ CAFs expressing an ORF vector for red fluorescent protein (pink dots) or with $CD146^{ORF}$ CAFs (purple dots). Invasion was measured for each sphere as described in the methods section and illustrated in Supplemental Figure 4. MCF-7 invasion was not significantly different between $CD146^{ORF}$ CAFs or with either $CD146^{neg}$ CAF group, which each had no expression for CD146, ns = not significant. An unpaired t-test was used to determine statistical significance using GraphPad Prism 8.3.0 and defined as $p < 0.05$; scale bars are 500μm.

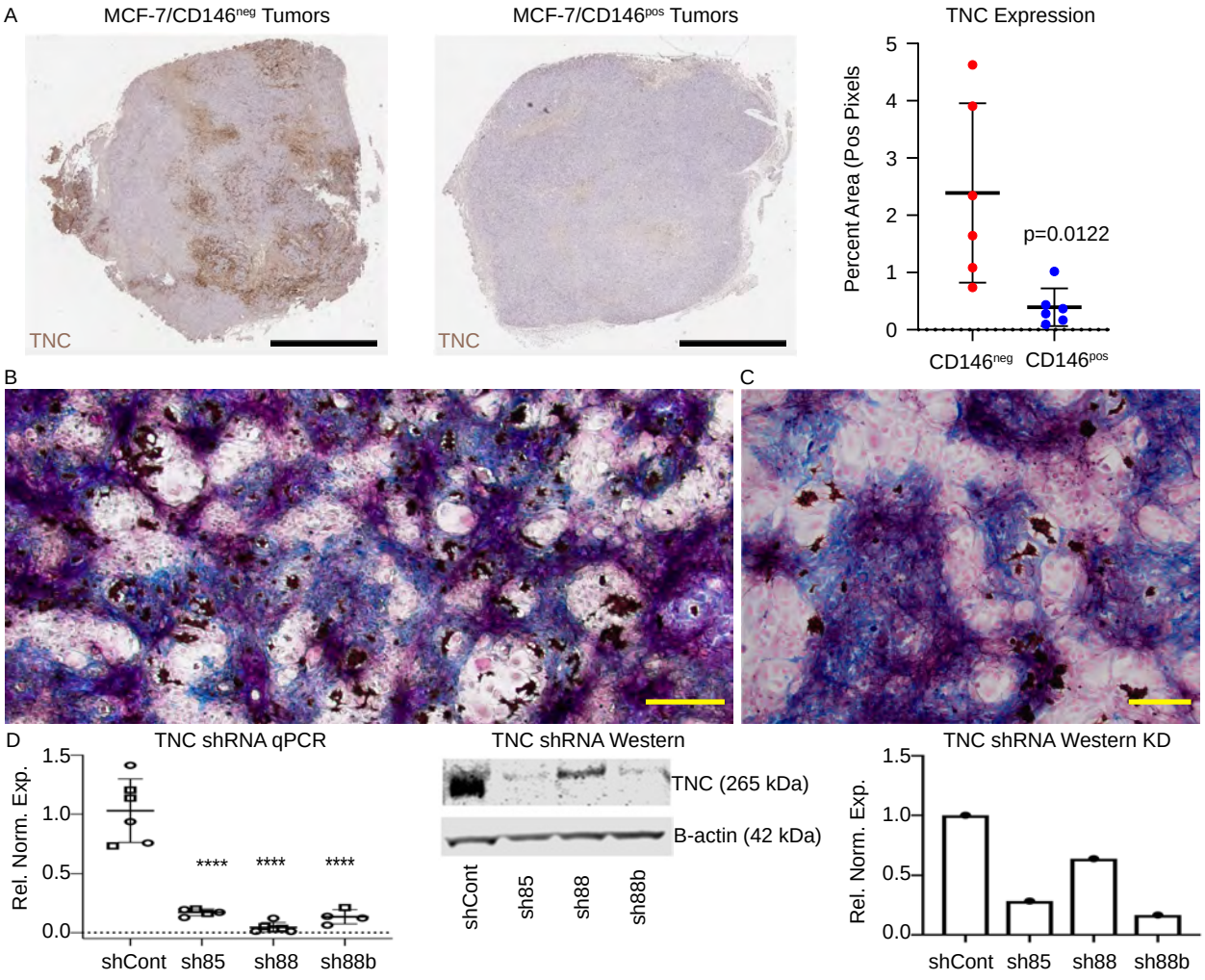

Supplemental Figure 3. TNC is expressed more in tumors with CD146^{neg} CAFs. (A) Immunohistochemistry for human specific TNC showed that MCF-7 tumors bearing CD146^{neg} CAFs expressed significantly more TNC compared to tumors with CD146^{pos} CAFs. Representative (B) 10X and (C) 20X images of a 72 hour co-culture of MCF-7 cells mixed with CD146^{neg} and CD146^{pos} CAFs. The cultures were stained using IHC methods for CDCP1 (blue stain marking CD146^{neg} CAFs), pan-cytokeratin (brown marking MCF-7 cells), TNC (purple) and Nuclear Fast Red (used to highlight presence of CD146^{pos} CAFs). TNC staining is strictly confined to areas populated by CD146^{neg} CAFs. Scale bars are 400μm and 200μm respectively. (D) qPCR and western blot analysis shows significant knockdown of TNC by shRNA in three different knockdown cell lines. TNC expression was analyzed by an unpaired t-test and TNC shRNA qPRC was analyzed with ordinary one-way ANOVA followed by Dunnet's multiple comparisons test. Scale bars = 2cm. ****p<0.0001.

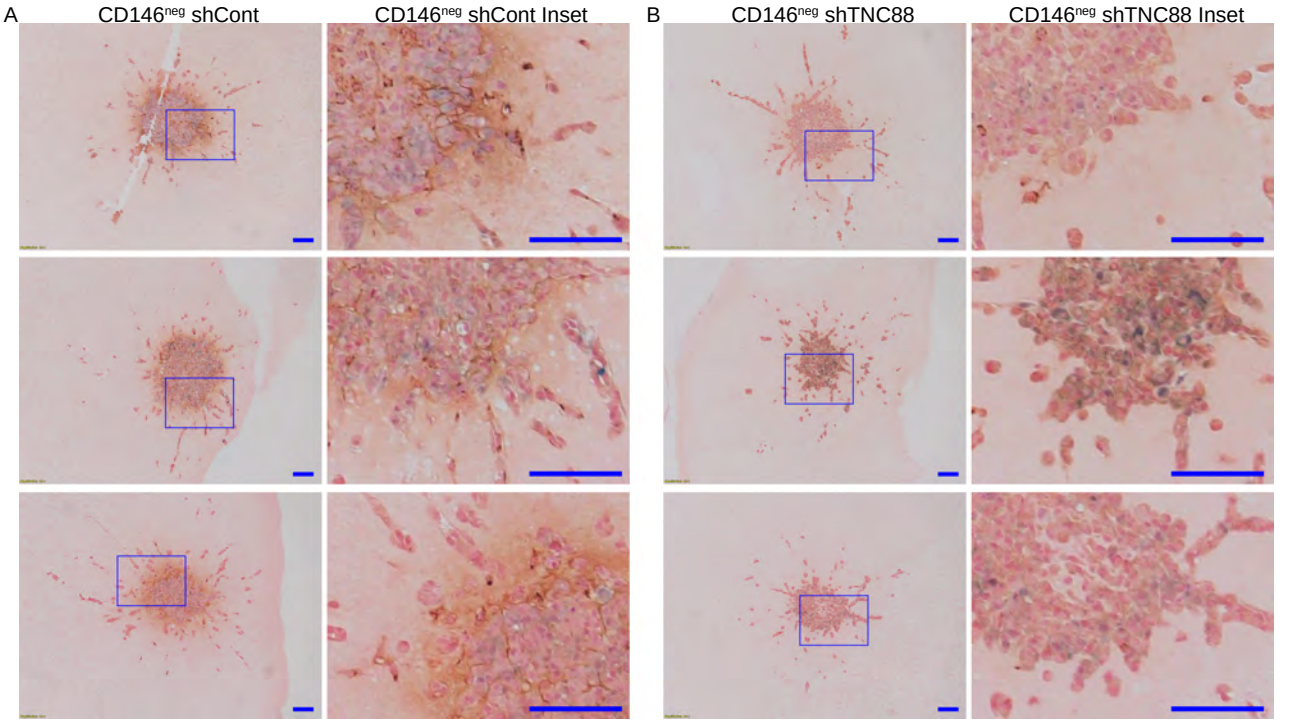

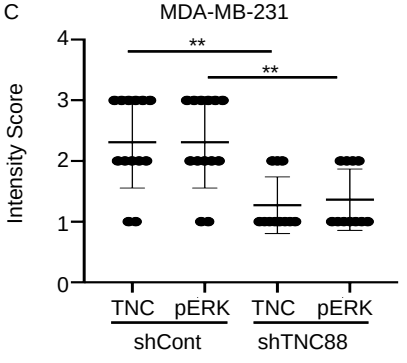

Supplemental Figure 4. MDA-MB-231 spheroid invasion fronts expressing TNC have significantly more pERK expression. MDA-MB-231 spheroids were co-cultured with CD146^{neg} CAFs expressing (A) control shRNA or (B) shRNA against TNC. Immunohistochemistry for phospho-ERK (pERK, blue) and TNC (brown) in 3 representative spheroids and counterstained with Nuclear Fast Red. Insets are marked by a blue box. (C) Intensity scores on a scale of 1-3 (1 = minimal staining, 2 = moderate staining, 3 = intense staining) for pERK and TNC. 4-6 serial images were scored per spheroid with N = 3 spheroids per group. Scale bars are 100μm. ****p<0.0001; statistics were completed using an ordinary 1-way ANOVA followed by Tukey's multiple comparison test.

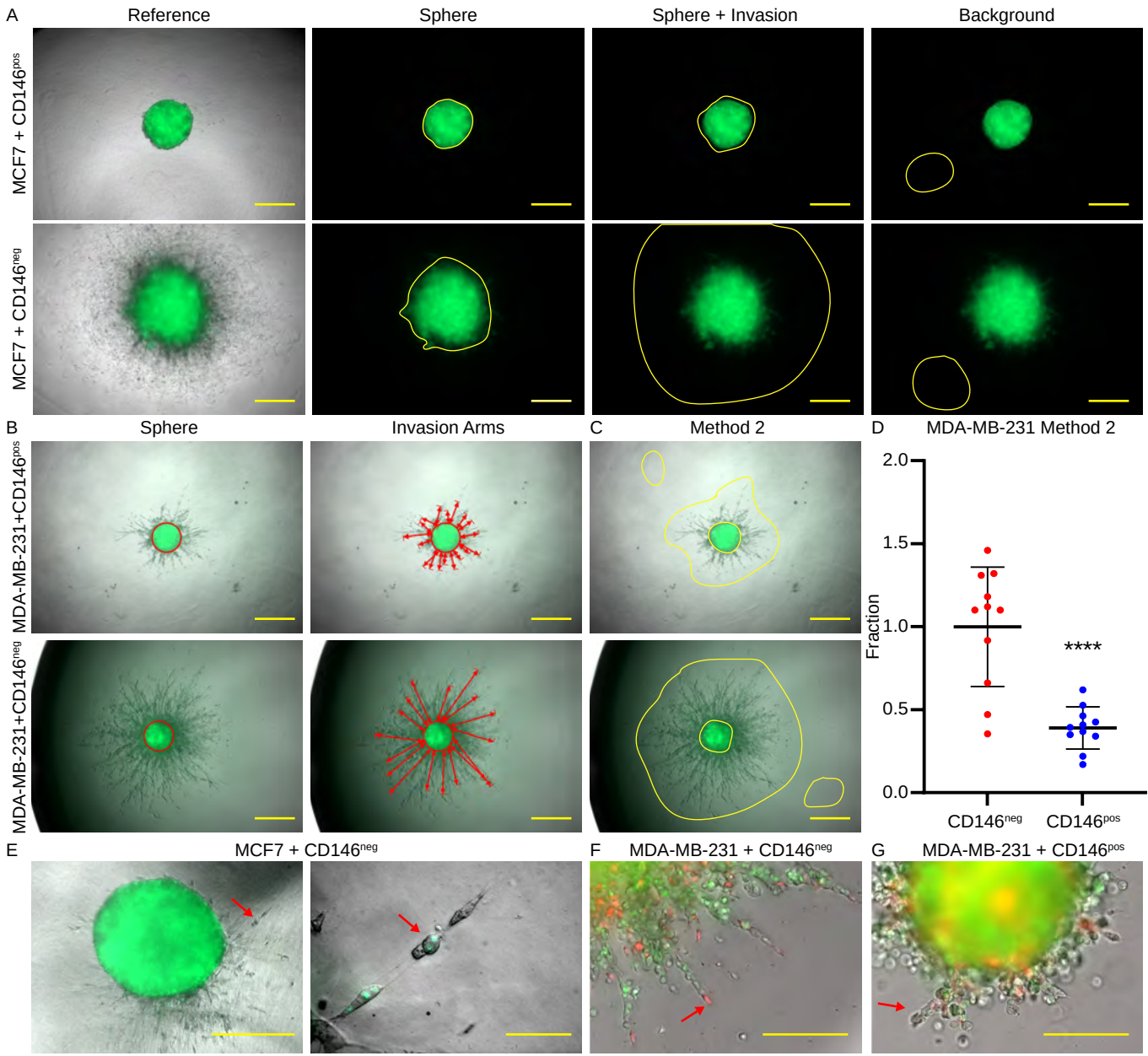

Supplemental Figure 5. Illustration of how spheroid invasion was quantified. Refer to the manuscript methods section for a detailed description on the methods used to measure invasion in the co-culture spheroid assays. (A) Representative image series showing how invasion for unlabeled CAF co-cultured spheroids mixed with GFP-labelled MCF-7 cells was measured. (B) Representative image series showing how invasion for CAF co-cultured spheroids mixed with GFP-labelled MDA-MB-231 cells was measured. (C) Re-analysis of the image series in panel B using the method described for MCF-7 spheroids. (D) Quantification of MDA-MB-231 invasion in co-cultures with CAF subtypes which were re-analyzed using the method for MCF-7 spheroids to demonstrate the consistency between methods used for MDA-MB-231 spheroids and to validate the method used for MCF-7 spheroids. (E) MCF-7/CD146^{neg} CAF co-cultured spheroid at 10X magnification and a single arm at 40X magnification. (F-G) High resolution images captured at 20X for GFP-labelled MDA-MB-231 cells co-cultured in spheroid assays with (F) RFP-labelled CD146^{neg} CAFs or (G) RFP-labelled CD146^{pos} CAFs. Arrows indicate invasion arms comprised of CAFs and MDA-MB-231 cells with several arms of the MDA-MB-231/CD146^{neg} CAF spheroid co-culture being tipped by CAFs. Scale bars are 500μm (A, B, C, E) and 200μm (F-G); N = 11 spheroids analyzed in each group, statistical analysis was done by unpaired t-test using GraphPad Prism 8.3.0.; **** = $p < 0.0001$. Disclosure: The Reference panels for MCF7 + CD146^{pos} and MCF7 + CD146^{neg} in A of this figure are repeat images, previously shown in the main text Figure 10A panels for MCF-7/CD146^{neg} and MCF-7/CD146^{pos}. Panels F (MDA-MB-231 + CD146^{neg}) and G (MDA-MB-231 + CD146^{pos}) in this figure are higher magnification images previously shown in the main text Figure 6B. The images in panels F and G have been rotated in comparison to the main text Figure 6B images.

Supplemental Table 1. ECM proteins expressed significantly different in MCF-7 tumors with $CD146^{neg}$ versus $CD146^{pos}$.

Human Specific Protein	**FC ($CD146^{neg}$ vs $CD146^{pos}$)**	**p-value**
Agrin	$CD146^{pos}$	--
Collagen alpha-1(XVIII) chain	0.51	0.014
Thrombospondin-1	0.46	0.009
Biglycan	8.35	0.034
Brevican core protein	2.70	0.028
Collagen alpha-1(IV) chain	$CD146^{neg}$	--
Collagen alpha-1(VI) chain	10.11	0.021
Collagen alpha-2(I) chain	14.84	0.031
Collagen alpha-2(VI) chain	12.15	0.021
Collagen alpha-3(V) chain	$CD146^{neg}$	--
Decorin	$CD146^{neg}$	--
EMILIN-1	$CD146^{neg}$	--
Extracellular matrix protein 1	$CD146^{neg}$	--
Fibrillin-1	$CD146^{neg}$	--
Fibronectin	50.37	0.001
Latent-transforming growth factor beta-binding protein 1	5.19	0.022
Latent-transforming growth factor beta-binding protein 2	$CD146^{neg}$	--
Tenascin-C	21.18	0.002
Shared Protein	**FC ($CD146^{neg}$ vs $CD146^{pos}$)**	**p-value**
Asporin	0.35	0.018
Basement membrane-specific heparan sulfate proteoglycan core protein	0.52	0.049
Biglycan	0.44	0.043
Collagen alpha-1(I) chain	0.28	0.018
Collagen alpha-1 (IV) chain	0.35	0.025
Collagen alpha-(V) chain	0.40	0.027
Collagen alpha-1(VI) chain	0.35	0.014
Collagen alpha-1(XVIII) chain	0.49	0.004
Collagen alpha-1/5(IV) chain (Arresten/Core Protein)	0.47	0.001
Collagen alpha-2(I) chain	0.30	0.013
Collagen alpha-2(VI) chain	0.38	0.002
Collagen alpha-2(V) chain	0.39	0.019
Collagen alpha-2(VI) chain	0.47	0.048
Dermatopontin	0.38	0.024
Fibromodulin	0.35	0.010
Laminin subunit alpha-1	$CD146^{pos}$	--
Laminin subunit beta-1	0.08	0.055
Laminin subunit beta-2	0.28	0.011
Laminin subunit gamma-1	0.11	0.046
Lumican	0.38	0.023
Mimecan	0.28	0.007
Nidogen 1/2 (osteonidogen)	0.16	0.024
Nidogen-1	0.16	0.019
Prolargin	0.29	0.016
Thrombospondin-1	0.47	0.027
Thrombospondin-2	0.66	0.021

Transglutaminase 2	0.43	0.051
Fibronectin 1	2.99	0.002
Fibronectin 1 (Anastellin/type-III domain)	2.75	0.001
Fibronectin 1 (type-III 13 domain)	12.86	0.004
Fibronectin 1 (type-III 4 domain)	65.07	0.001
Fibronectin 1 (type-III 7 domain)	2.81	0.003
Fibronectin 1 (type-III 9 domain)	1.64	0.031
Fibulin-1	1.48	0.029
Latent-transforming growth factor beta-binding protein 1	$CD146^{neg}$	--
Lysyl oxidase	$CD146^{neg}$	--
Vimentin	3.21	0.020
Mouse Specific Protein	**FC ($CD146^{neg}$ vs $CD146^{pos}$)**	**p-value**
Basement membrane-specific heparan sulfate proteoglycan core protein	0.45	0.017
Biglycan	0.41	0.043
Collagen alpha-1(IV) chain	0.36	0.003
Collagen alpha-1(VI) chain	0.31	0.016
Collagen alpha-1(XVIII) chain	0.49	0.020
Collagen alpha-2(VI) chain	0.44	0.001
Collagen alpha-3(IV) chain	0.38	0.003
Collagen alpha-3(VI) chain	0.35	0.015
Decorin	0.20	0.018
Dermatopontin	0.40	0.025
Galectin-7	$CD146^{pos}$	--
Insulin-like growth factor-binding protein 7	0.35	0.006
Laminin subunit alpha-1	$CD146^{pos}$	--
Laminin subunit beta-2	0.31	0.033
Laminin subunit gamma-1	0.08	0.049
Lumican	0.43	0.042
Mimecan	0.33	0.003
Nidogen-1	0.11	0.037

Fold change normalized to total protein expression. $CD146^{pos}$ = only detected in tumors with $CD146^{pos}$ CAFs; $CD146^{neg}$ = only detected in tumors with $CD146^{neg}$ CAFs.

Supplemental Table 2. ECM proteins used to generate the gene signature predictive of lymph node involvement.

	Observed vs Expected Lymph Node Metastasis					
Gene (individual)	T1 obs/exp	T1 pval	T2 obs/exp	T2 pval	T3 obs/exp	T2 pval
human isoform						
COL6A1	0.148	0.203	0.089	0.105	-0.015	1.000
COL5A2	0.110	0.372	0.064	0.256	-0.015	1.000
FN1	0.110	0.372	0.035	0.570	-0.089	0.343
BGN	0.127	0.307	0.127	0.019	0.045	0.704
COL1A2	0.175	0.126	0.127	0.019	-0.046	0.704
TGFBI	0.105	0.372	0.013	0.871	-0.212	0.022
COL6A3	0.228	0.041	0.163	0.002	-0.110	0.254
COL5A3	0.253	0.022	0.047	0.417	-0.046	0.704
FBN1	0.175	0.126	0.107	0.051	-0.046	0.704
LTBP2	0.180	0.125	0.148	0.006	-0.015	1.000
EMILIN1	0.159	0.162	0.122	0.023	-0.015	1.000
DCN	0.138	0.251	0.110	0.042	-0.015	1.000
shared isoform						
LOX	0.164	0.107	0.107	0.051	-0.015	1.000
Gene Signature (total)	0.268	0.015	0.148	0.006	-0.110	0.254